Time-resolved photoelectron spectroscopy of low-energy excitations of 4×4 C_{60}/Cu(111)

Arne C. Rosenfeldt,[a] Benjamin Göhler, and Helmut Zacharias
Physikalisches Institut, Westfälische Wilhelms-Universität, Wilhelm Klemm Str. 10, 48149 Münster, Germany

(Received 3 August 2010; accepted 15 November 2010; published online 20 December 2010)

Time-resolved two-photon photoemission is applied to investigate electron dynamics in multiple monolayers (MLs) of ordered fullerite on a copper substrate. The experimental data are analyzed assuming coupled excited state dynamics. Rate equations fitted to these dynamics yield lifetimes of about 80 ps for the lowest unoccupied molecular orbital (LUMO), about 1.2 ns for the singlet exciton and 22 μs for the triplet exciton at a surface temperature of 140 K. For trapped triplet excitons lifetimes up to 200 μs are observed. An increased excitation fluence reduces the lifetime of the excitons due to annihilation. An increased sample temperature slightly reduces the lifetime of the triplet exciton. There is no evident dependence of the exciton lifetimes on the pump photon energy in the range of $h\nu = 2.9$ to 3.3 eV. A dependence on the layer thickness (10–20 ML) is not observed as long as more than 9 ML are prepared. © *2010 American Institute of Physics*. [doi:10.1063/1.3524313]

I. INTRODUCTION

The properties of the low-lying electronic states in C_{60} thin films have important implications for the behaviour of fullerene films in various applications, like photovoltaic devices, transmission sensitive coatings, and molecular electronics. Here the energy transfer into acceptor states in functionalized C_{60} is important.[1,2] Many experiments have been devoted to clarify the energetic position of electronically excited lowest unoccupied molecular orbital (LUMO) states and the lowest singlet and triplet excitons relative to the highest occupied molecular orbital (HOMO) on various substrates.[3,4] Depending on the substrate the energetic position of the lowest LUMO and those of the excitons in the first C_{60} layer is below or above the Fermi energy, thereby changing the degree of metallic character. This behaviour also has influence on the ability to act as an electron acceptor for further adsorbates. In particular the dynamics of these states influence the photophysical and photochemical response of bare and functionalized fullerene films after excitation in certain photon energy bands.

Ordered C_{60} thin films or fullerite is a solid with only weakly interacting van der Waals forces between the constituents. Therefore, the electronic properties become to a certain extent already apparent in gas phase or matrix isolated entities. Of course, the solid features specific properties not available for single C_{60} molecules, like a high electron mobility by hopping,[5] diffusion of excitons and, at high densities, exciton – exciton annihilation.[6] Further, for adsorbate covered C_{60} films a chemical interaction with electronic states of the adsorbate may occur.

In ideal, nonvibrating and nondeformed C_{60} the electronic transition from the HOMO to the LUMO with a band center energy difference of about 2.2 eV is electric dipole forbidden due to the symmetry of the states. At somewhat higher photon energies the LUMO+1←HOMO and the LUMO←HOMO-1 transitions become dipole allowed, thereby enabling effective excitation with the second harmonic of a Ti:sapphire ($\lambda \sim 400$ nm),[7–11] the third harmonic of a neodymium laser ($\lambda = 355$ nm)[12] and the radiation of a XeCl excimer laser.[13] However, in crystalline C_{60} the absorption of photons with an energy of 2.33 eV ($\lambda = 532$ nm)—the second harmonic of a neodymium laser—and thus in the LUMO ← HOMO transition, is significantly more effective than in the gas phase or in a nonpolar matrix due to a symmetry reduction by an initial state with non-zero wave vector.[14] Further, the electron delocalization across the crystal causes electronic band formation with a width of about 0.4 eV.[15–17]

Bound electron–hole pairs or excitons exist in fullerite as well as in the gas phase or in matrix isolated C_{60} molecules. In the latter case they are naturally localized, in fullerite excitons may diffuse through the bulk, but may also appear at the surface. Excitons can exist in singlet and triplet spin configurations. Sawatzky and co-workers showed that singlet excitons can resonantly be excited from the HOMO by photons with about 1.826 eV energy ($\lambda \sim 679$ nm),[18] in agreement with an earlier photoconductivity measurement.[19] Using electron energy loss spectroscopy (EELS) Gensterblum *et al*. observed the triplet exciton in fullerite at energies about 1.5 eV above the HOMO state.[20]

Previously, several investigations were concerned with the decay of electronic excitations, both in the single electron states as well as in excitonic states. However, a broad variation of lifetimes and decay rates has been reported. It is generally agreed that electrons in the LUMO+1 relax within a ps or less into the LUMO state, depending on the thickness of the film due to charge diffusion and on the substrate.[7,8,11] At a film thickness larger than 1 nm a classical dipole—dipole damping mechanism prevails.[21] Electrons in the LUMO then decay with lifetimes between less than 20 ps in matrix isolated C_{60}[10] and 134 ps in fullerite[7] into the singlet exciton.

[a]Author to whom correspondence should be addressed: arnero@uni-muenster.de.

The singlet exciton relaxes by spin-orbit interaction nearly resonantly into the triplet exciton state,[22] because it can not decay into the HOMO via electric dipole radiation. Using various methods and systems lifetimes between 33 ps and 1.3 ns have been reported.[6,7,21–23] Branching ratios for exciton relaxation and free carrier generation between 35% and 100% are reported.[6,24]

Due to the necessary spin flip the lowest triplet exciton relaxes into the ground state only at very low rates. In ultracold, matrix isolated C_{60} molecules lifetimes of the triplet exciton between 16 μs and 470 μs have been measured by phosphorescence[25,26] or ESR.[23,27] In gas phase experiments lifetimes of the triplet exciton between 30 ns and 3 μs have been observed.[12,28] The lifetimes depend on the amount of vibrational excitation and thus vibronic coupling with other states. At temperatures of 81 K Kabler and co-workers reported lifetimes of 15 μs for photopolymerised fullerite.[6] They also observed that at laser fluences above 0.1 mJ/cm^2 singlet exciton annihilation and above 1 mJ/cm^2 triplet exciton annihilation become major decay channels.

In the present investigation ordered (4×4) C_{60} layers are grown on Cu(111). Previously, Osterwalder and co-workers[29] observed with angle-resolved ultraviolet photoemission for one monolayer (ML) of C_{60} on Cu(111) a transformation of the Shockley surface state of Cu(111) into an interface state between Cu(111) and fullerite. A second interface state develops at about 1 eV below E_F due to a hybridization between the six carbon atoms facing the copper surface and the first few layers of copper atoms, as theoretical calculations suggest. According to this calculation on average 0.8 electrons are transferred from the copper to each C_{60} molecule adsorbed in the first ML, whereas according to their experiment on average 2.9 electrons are transferred from the copper to each C_{60} molecule adsorbed in the first ML. Similar results were found earlier by Tsuei and co-workers.[30,31] On average between 0.8 and 2.0 electrons are transferred to the C_{60} molecules of the first ML. Theoretical calculations of the electron redistribution for the adsorption of one ML on noble metals yield the conclusion that about one charge is localized between the metal surface and the carbon atoms of C_{60}.[32,33] Upon further growths of additional ML the film then shows the properties of bulk fullerite. Employing two-photon photoemission the energetic position of excitonic states and of single electron excitations are measured. Introducing a time delay between a wavelength tunable pump pulse and a probe pulse reveals the excited state dynamics in both the time and state energy domain.

II. EXPERIMENTAL

An ultra-high vacuum (UHV) chamber with a base pressure of $5 \cdot 10^{-10}$ mbar equipped with an internal μ-metal shield is employed. A copper (111) single crystal with 10 mm diameter is used as substrate. The crystal is introduced into the chamber, sputter annealed, and checked for cleanness by means of Auger spectroscopy, low energy electron diffraction (LEED) and PES. The C_{60} films are prepared by vapour deposition. A molybdenum crucible containing C_{60} powder (99.9%+ purity; Proteomics) is heated by an electron beam. After outgassing the evaporator for one hour, the pressure in the vacuum chamber stays below 10^{-9} mbar. At a temperature of 700 K C_{60} shows a vapour pressure of $3.6 \cdot 10^{-2}$ mbar.[34,35] The molecules evaporate through a hole in the crucible and are guided by a metal tube to be deposited onto the copper crystal held at a temperature of 363 K. Some molecules become ionized by the electron beam and hit the tube. Monitoring this positive ion current allows to reproducibly prepare C_{60} films. Typically, at a current of 0.5 nA one ML is grown in 230 s. After deposition of a few ML the copper crystal is heated to a temperature of 600 K which leads to desorption of all but the first ML and induces a long-range order in this first monolayer. Then further C_{60} is evaporated up to 20 ML at a temperature of 363 K. This procedure ensures an ordered growth of a (4×4) C_{60} film on the Cu(111) surface, as is verified by LEED.

For excitation and photoemission spectroscopy (PES) a tunable OPO/OPA laser pumped by a mode-locked Nd:YLF laser is used. The system has been described in detail previously.[36–38] At a repetition rate of 1 kHz pulse energies of up to 500 μJ tunable in the range from 1460 to 1740 nm are available. Two consecutive LBO crystals are used to generate the fourth harmonic, yielding radiation tunable in the range from $\lambda = 365$ to 435 nm ($h\nu = 3.40$ to 2.85 eV) with about 20 μJ pulse energy. The pulses travel over a translation stage to synchronize them with the probe pulses, and are used to excite the C_{60} film. From the partly depleted fundamental pulse of the Nd:YLF laser the second ($h\nu = 2.35$ eV, $\lambda = 526.5$ nm), fourth ($h\nu = 4.71$ eV, $\lambda = 263.25$ nm) and fifth ($h\nu = 5.88$ eV, $\lambda = 210.6$ nm) harmonic are generated in consecutive BBO crystals to generate the probe laser pulses. Further, the seventh harmonic ($h\nu = 8.24$ eV, $\lambda = 150.4$ nm, 10^4 photons per pulse) of the Nd:YLF laser is available by third order nonresonant difference frequency mixing in Xe gas ($p \sim 60$ mbar) the fourth harmonic with the fundamental pulse.[39,40] For time delays in the microsecond range a second laser is used which permits to adjust the delay electronically. The third harmonic of a Q-switched Nd:YAG laser ($h\nu = 3.49$ eV, $\lambda = 355$ nm, pulse duration 120 ns) is employed. *P*-polarized laser pulses of 9 μJ energy focused to a fluence of 0.1 mJ/cm^2 are applied to the C_{60} film. Fig. 1 shows schematically the experimental setup.

In the present experiment a lens weakly focuses the pump beam to an elliptic spot on the sample with an area of 0.25 mm^2 leading to fluence of up to 0.1 mJ/cm^2. The laser radiation impinges under an angle of $\vartheta = 60^\circ$onto the sample, see Fig. 1. The probe beam spot size and position is adjusted to be spatially within the pump beam spot. For this alignment a camera is directed at a screen covered with fluorescent zinc silicate temporarily replacing the sample. The laser pulses are *p*-polarized incident on the sample surface. To separate the time-resolved two-colour photoelectron spectrum from the non time-resolved mono-colour one-photon PES (1PPE) and two-photon PES (2PPE) spectra, synchronized choppers are employed in both the pump and the probe beam, each blocking a quarter of the pulses. The choppers are time-shifted with respect to each other. Thus, three different PE spectra are recorded simultaneously, one produced by the pump, one by the probe, and the third by both laser pulses. Laser pulse

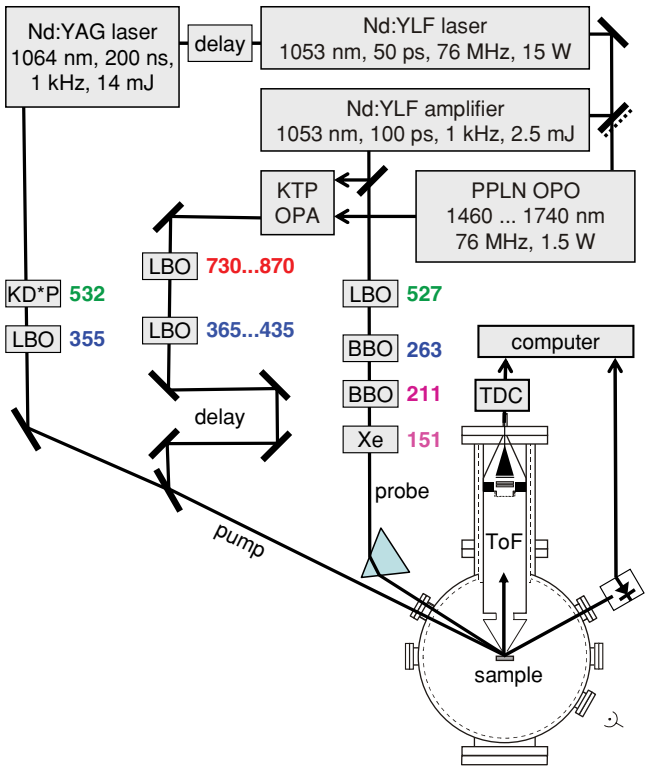

FIG. 1. Schematics of the experimental set-up, indicating the various frequency mixing steps in both the pump and probe beams. The angle of incidence of the *p*-polarized laser pulses on the sample ist 60°.

intensities are recorded from the reflections of the entrance window on a pulse-to-pulse basis. Photoelectrons emitted from the sample in normal direction are detected in a time-of-flight (ToF) spectrometer after a distance of 405 mm using a multi channel plate detector. Their time-of-flight is recorded by a time-to-digital converter (ACAM AM-GP1, 125 ps resolution) and stored in a computer. Typical spectra consist of 10^5 laser pulses per time delay setting. For optically delayed probe pulses time delay steps of $\Delta t = 33.35$ ps are used, for the electronically delayed ones the step size is increased to $\Delta t = 105.7$ ns over a total delay range of more than 25 μs.

The two-dimensional time-delay spectra are cut at certain energies to gain state dynamics, and vice versa the time-delay spectra are cut at certain delays to gain dynamic spectra. For the mechanical pulse delay line the states investigated are the singlet exciton (E) and the electrons in the LUMO. The resulting state dynamics are then fitted by a set of rate equations:

$$\frac{d}{dt}N_i(t) = 0, \tag{1}$$

$$\frac{d}{dt}N_E(t) = R_{E,i}(t)N_i(t) + \frac{-1}{\tau_E}N_E(t) + R_{E,\mathrm{LUMO}}N_{\mathrm{LUMO}}(t), \tag{2}$$

$$\frac{d}{dt}N_{\mathrm{LUMO}}(t) = R_{\mathrm{LUMO},i}(t)N_i(t) + \frac{-1}{\tau_{\mathrm{LUMO}}}N_{\mathrm{LUMO}}(t), \tag{3}$$

$$\frac{d}{dt}N_{f_0}(t) = R_{f_0,E}(t)N_E(t), \tag{4}$$

$$\frac{d}{dt}N_{f_1}(t) = R_{f_1,\mathrm{LUMO}}(t)N_{\mathrm{LUMO}}(t). \tag{5}$$

Here N are the numbers of electrons in the respective states. In addition to the already mentioned states the theory of two-photon photoemission contains the initial state [i, Eq. (1)] and the final states [f_0 in Eq. (4) and f_1 in Eq. (5)]. R are rates between the states, some of which depend on the time delay t because they represent photo excitation by either the pump [Eqs. (2) and (3)] or the probe pulse [Eqs. (4) and (5)]. Two rates are replaced by the respective lifetimes τ_{LUMO} and τ_E. In Eq. (1) the nondepletion approximation is applied. Some rates in Eqs. (2) and (3) are time-dependent, because they describe the excitation by the pump pulse which is assumed to be of Gaussian shape. Equations (4) and (5) describe photoemission into the final states due to the probe pulse, which is delayed with respect to the pump pulse. By writing this as a matrix equation $\frac{d}{dt}N(t) = R(t) \cdot N(t)$ and transforming into the frequency domain a good numerical approximation to the solution can be obtained.

III. RESULTS AND DISCUSSION

A. Spectra

Figure 2 shows photoemission spectra in normal direction from fullerite films of different thicknesses on Cu(111) at a temperature of 140 K recorded with a photon energy of $h\nu = 8.24$ eV. The thickness is calibrated by comparing the spectra to that obtained by annealing the film to the first

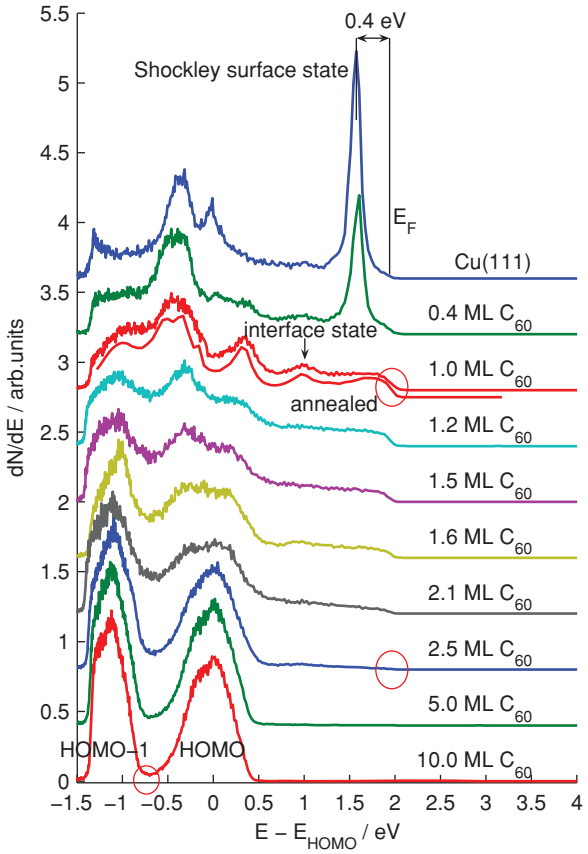

FIG. 2. Normal photoemission spectra from C_{60}/Cu(111) recorded for different film thickness; photon energy: $h\nu = 8.24$ eV, $\lambda = 150.4$ nm, $T_S = 140$ K. The red circles mark the Fermi edge and the high contrast between HOMO and HOMO-1 for well-prepared films.

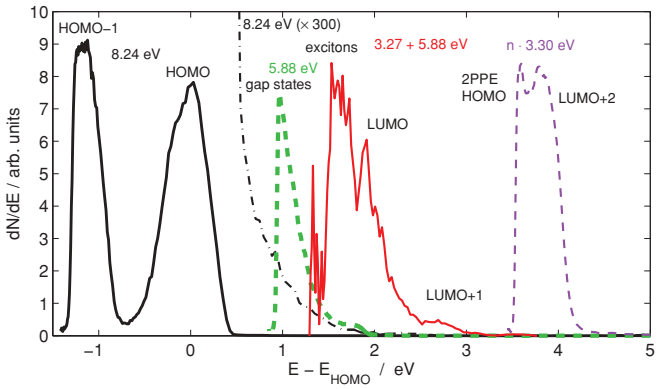

FIG. 3. Photoemission spectra of fullerite using various photon energies. The spectrum denoted (3.27 eV + 5.88 eV) is a background-subtracted pump-probe spectrum taken at zero delay. The position of the HOMO peak in the solid (black) curve is taken as energy reference.

ML and assuming a constant sticking coefficient upon further evaporation. The energy scale relates to the position of the HOMO state at a thick fullerite film. On clean copper features of the 3d band and the Shockley surface state at 0.4 eV below E_F can be recognized. The Fermi edge of Cu appears at $E = E_{HOMO} + 1.9$ eV. On the 1 ML thick C_{60} film an interface state evolves at $E - E_{HOMO} = 1.0$ eV, in agreement with results of Osterwalder and co-workers.[29] This weak peak becomes more visible upon annealing of the first ML, which is metallic as indicated by the appearance of a Fermi edge. At 2.5 ML C_{60} the Fermi edge vanishes. The HOMO-1 is located at $E - E_{HOMO} = -1.2$ eV, in agreement with previous results.[8,41,42] It should be noted that the HOMO-1 state is only partially observed due to the limited photon energy of 8.24 eV. The circle at 10 ML C_{60} marks the high contrast in the spectrum between the HOMO and the HOMO-1, indicative of a good preparation and the absence of photo polymerization. It should be noted that over the course of this work many samples with thicknesses between 10 and 20 ML have been prepared. Only those which show the indicated deep separation between HOMO-1 and HOMO are considered here. Upon C_{60} deposition the low energy cut-off in the spectrum, and thus the work function, stays constant within 0.1 eV of that of Cu(111) of (4.94 ± 0.03) eV,[43] a result also observed by Dutton and Zhu.[44] The first ML exhibits a 4×4 superstructure in LEED in agreement with earlier observations by Tsuei and Johnson.[30] Figure 2 shows that after a deposition of 10 ML the C_{60} thin film is well-developed and exhibits a bulk-like electronic structure.

Figure 3 shows combined photoemission spectra taken on more than 10 ML C_{60}/Cu(111) with different photon energies and one and two-colour excitations. They are placed on a single energy scale by subtracting the respective probe photon energy. The solid (black) curve, the dash-dotted (black) curve and the dashed (green) curve denote single-photon PE spectra taken with photon energies of 8.24 eV and 5.88 eV, respectively. The Fermi edge appears at 1.9 eV in agreement with earlier studies.[7,44] The solid (red) curve above 1 eV represents a 2-colour 2PPE spectrum taken with a pump photon energy of 3.27 eV and a probe photon energy of 5.88 eV from which the mono-colour (pump+pump and probe+probe) background is subtracted. Here the LUMO appears at 2.1 eV, just above the Fermi energy. The LUMO+1 can be discerned at 2.8 eV and the LUMO+2 appears at 4.0 eV (thin dashed magenta curve) in agreement with results reported by Dutton and Zhu.[11] The spectrum was taken with a photon energy of 3.3 eV. The peak at 3.5 eV is a 2PPE replica of the HOMO. Below the LUMO spectral signatures of the singlet and the triplet excitons overlap. Their energetic positions are in agreement with observations of Eberhardt and co-workers,[7] who reported that the singlet exciton leads to a peak in the PE spectrum at 1.8 eV above the HOMO, and Kabler and co-workers[6] reported that the triplet exciton is located 0.33 eV below the singlet exciton. The dip around 1.3 eV is interpreted as noise, which is quite large due to the large background subtracted. The dip does not separate the triplet exciton from the singlet exciton. The spectral signatures of the states observed are listed in Table I together with earlier literature data.

TABLE I. Energetic positions (in eV) of excited states in C_{60} crystals referenced to the highest occupied molecular orbital (HOMO). 2PPE: two-photon photoemission, TR-2PPE: time-resolved 2PPE, EELS: electron energy loss spectroscopy, AS: absorption spectroscopy, SFG: sum frequency generation, PC: photoconductivity, PS: photoluminescence spectroscopy, TRPS: time-resolved PS, IPE: inverse photoelectron spectroscopy. The Fermi energy is determined to be at 2.18 eV[a,b] for C_{60} on copper, which is below the lowest unoccupied molecular orbital (LUMO). The LUMO+2 is found at 4.0 eV.[a,d] The transition from the HOMO-1 to the LUMO is visible in AS at 2.7 eV[s]. In the present investigation the Fermi energy is found to be at 1.9 eV. The LUMO+2 is observed at 3.9 eV. The HOMO-1 is visible in PES 1.2 eV below the HOMO (see Figs. 2 and 3). The work function of thick C_{60} films on Cu(111) is 4.95 eV[t].

Exciton				
Triplet	Singlet	LUMO	LUMO+1	Method, Publication
	1.9	2.2	3.0	TR-2PPE[a]
1.55	1.8	2.2	3.0	TR-2PPE[b]
1.54	1.87	2.0		TR-2PPE[c]
			2.87	2PPE[d]
1.55	1.8	2.2		EELS[e]
1.54				EELS[f]
	2.3	2.7		AS[g]
	1.83			SFG[h]
	<1.99	<2.36		PC[i]
	1.85	2.5		PC[j]
1.6		2.25		PC[k]
		2.35	3.5	PC, PS[l]
	1.871			PS[m]
1.50				TRPS[n]
1.45	1.6			TRPS[o]
		2.3	3.4	IPE[p]
1.30	1.58	2.5		theory[q,r]
1.45	1.8	2.1	2.8	present work
0.4	0.7	0.5	0.3	energetic width

[a]Reference 8.
[b]Reference 7.
[c]Reference 9.
[d]Reference 11.
[e]Reference 45.
[f]Reference 46.
[g]Reference 47.
[h]Reference 48.
[i]Reference 19.
[j]Reference 49.
[k]Reference 50.
[l]Reference 51.
[m]Reference 52.
[n]Reference 53.
[o]Reference 54.
[p]Reference 41.
[q]Reference 55.
[r]Reference 56.
[s]Reference 14.
[t]Reference 44.

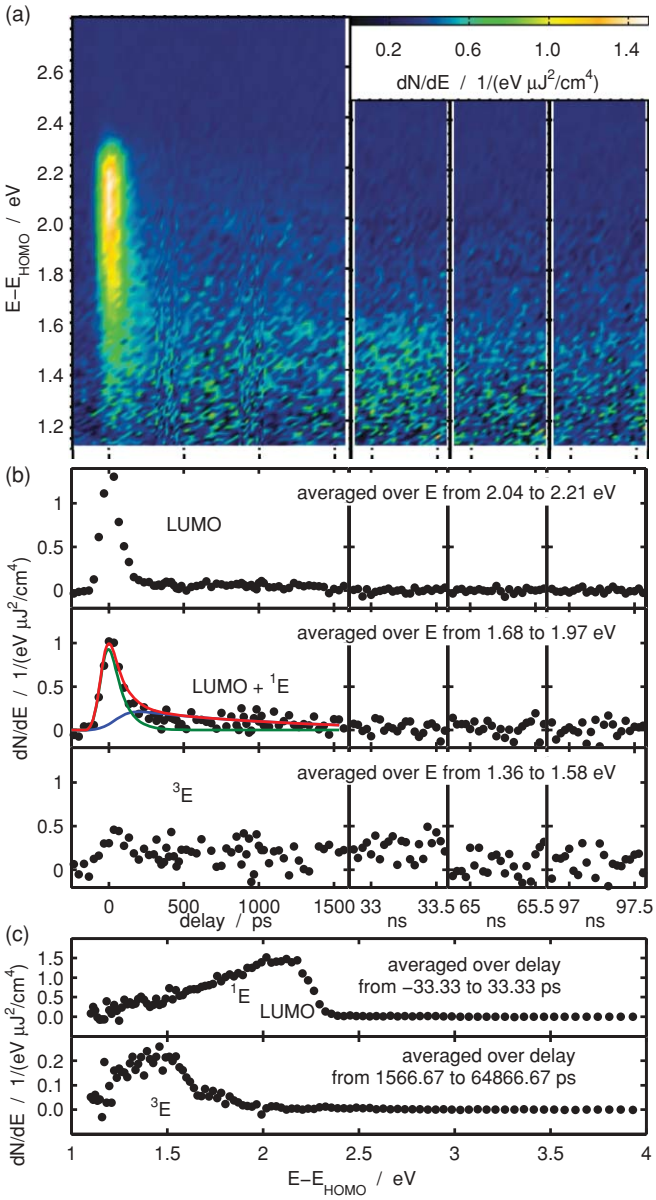

FIG. 4. (a) Energy-time delay plot of two-colour 2PPE spectra. Pump photon energy: $h\nu = 2.35$ eV ($\lambda = 527$ nm), fluence = 0.044 mJ/cm^2; probe photon energy: $h\nu = 5.88$ eV ($\lambda = 211$ nm), fluence: 1 nJ/cm^2, film thickness: 14 ML. (b) Cuts through the plot at three different energy intervalls: 2.21–2.04 eV representing the LUMO, 1.97–1.68 eV a mixture of LUMO and singlet exciton (^{1}E), and 1.58–1.36 eV showing the triplet exciton (^{3}E). In the middle trace the averaged signal is fitted by a superposition of two states with lifetimes of 80 ps (LUMO) and of about 1020 ps (singlet exciton). (c) Energy distributions at two different time delays. The upper one shows the rapid population of the LUMO and the ^{1}E, the lower one represents the ^{3}E.

B. Dynamics

Figure 4 shows an energy versus time-delay spectrum up to delays of 97.5 ns taken with a pump photon energy of 2.35 eV ($\lambda = 526.5$nm) at a fluence of 0.044 mJ/cm^2 and a probe photon energy of 5.88 eV ($\lambda = 211$ nm). The state energy above HOMO is plotted as a function of probe photon delay time. The intensity is color-coded, as given by the inset. The probe photon energy of 5.88 eV is too small to directly emit electrons out of the HOMO or HOMO-1 states.

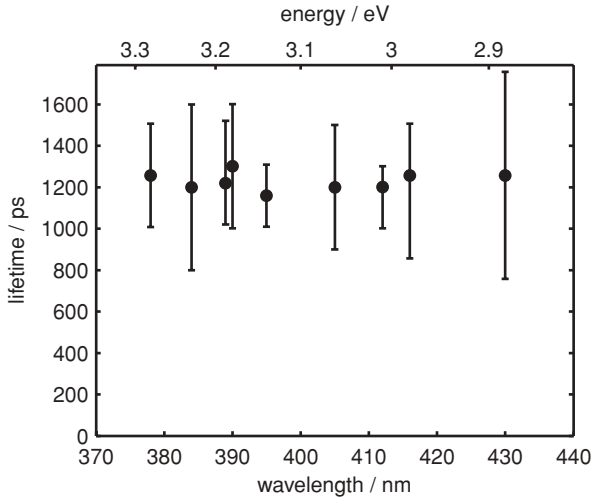

FIG. 5. Measured singlet exciton lifetimes for different pump photon energies from 2.85 to 3.29 eV. An average lifetime of (1230 ± 100) ps is deduced. Measurements with different fluences show that at high fluence the lifetime shortens.

The spectrum extends from the low energy cutoff at about 1.3 eV to the pump photon energy at 2.35 eV. The LUMO peaks at 2.1 eV, which is visible in the spectrum at short delays (from −30 ps to 100 ps), and which is in agreement with the reported observations for the LUMO in Table I. The singlet exciton is centred at 1.8 eV, which also agrees with reported values for the singlet exciton in Table I. The lowest triplet exciton is centred at 1.45 eV and has a FWHM of 0.4 eV as is visible in the spectrum at large delays.

The signal averaged over the energy from 1.68 to 1.97 eV is fitted by a superposition of state dynamics, one with a short lifetime of 80 ps, which represents the LUMO state, and one with a longer lifetime of about 1020 ps, which is interpreted as the lifetime of the singlet exciton. The measured lifetime of the LUMO is smaller than the value of 134 ps reported by Eberhard and co-workers,[7] but close to that observed by Kuhnke *et al.*[57] of 70 ps. Eberhard and co-workers[8] found that for well-developed C_{60} films the lifetime is unaffected by film thickness. The lifetime of 25 ns reported by Kabler and co-workers[6] for the LUMO does not fit with other observations. They investigated polymerized C_{60}. In their spectra only the singlet and triplet excitons are visible, and the LUMO lifetime was concluded from rate equations set up to explain the observed increased triplet to singlet exciton intensity ratio with increased pump fluence.

For a deeper understanding of the singlet exciton lifetime we performed experiments with other pump photon energies between $\lambda = 430$ nm and 375 nm ($h\nu = 2.88$ and 3.30 eV). Figure 5 shows the lifetimes observed for several different preparations. No obvious variation of the lifetime is found. This may be rationalized by the fact that after direct optical pumping of the LUMO the energy relaxes directly to the lowest singlet exciton state. Therefore, the averaged value of $\tau = (1230 \pm 100)$ ns observed at different pump photon energies may yield a better estimate of the lifetime of the singlet exciton. This average lifetime of the singlet exciton agrees better with those reported by Kabler and co-workers,[6] who determined 1.3 ns, than with those of Eberhardt and

co-workers[7] who measured 998 ps. It is thus likely that in the specific measurement shown in Fig. 4 the apparent lifetime might be reduced by inelastic singlet-singlet collisions due to the high fluence. And indeed varying the fluence, we observe that for a pump photon energy around 3.1 eV (400 nm) at a fluence of 0.05 mJ/cm^2 half of the singlet excitons decay due to inelastic singlet-singlet collisions, as discussed in detail by Kabler and co-workers.[6] A condensation into a free electron-hole liquid, as, e.g., is observed at high excitation densities in diamond,[58] seems not to occur. This suggests that the excitons remain rather localized on the individual C_{60} constituents of the film. It should be noted that the peak signal of the singlet exciton is delayed by 30 ps with respect to the LUMO, which reaffirms that the lowest singlet exciton state is populated by the decay of energetically higher states.

In Fig. 4 the lowest triplet exciton shows a lifetime which is longer than the maximum delay of 97.5 ns achieved by optically delaying the probe pulse. Therefore, we employed a second laser to achieve longer time delays by electronically delaying both lasers with respect to each other. Figure 6 shows an energy versus time-delay spectrum which is obtained by using a pump photon energy of $h\nu = 3.49$ eV ($\lambda = 355$ nm) and a probe photon energy of $h\nu = 5.88$ eV ($\lambda = 211$ nm). Again, the state energy above HOMO is plotted versus probe delay of up to $\Delta t = 26$ μs. The signal around 1.8 eV is due to the singlet exciton. A state at 1.45 eV is interpreted as the triplet exciton. The signal between 1.1 eV and 1.3 eV is interpreted as trapped excitonic states of C_{60}. The energetic position of this triplet exciton is in agreement with the reported values in the literature, see Table I.

The state dynamics of the triplet exciton can be fitted by a superposition of two exponential decays, one with a lifetime of (720 ± 50) ns and one with a lifetime of (22.3 ± 0.6) μs. The larger lifetime is in rough agreement with the value of 15 μs reported by Kabler and co-workers.[26] They explained the appearance of a short lifetime by triplet-triplet annihilation.

The thickness of the fullerite film is varied from 10 ML to 17 ML. From the measured small variation of triplet exciton lifetimes we estimate that for these thicknesses most triplet excitons decay spontaneously and less than every tenth triplet exciton decays due to a collision with the interface to the substrate. From a series of spectra taken on a sample while it heats up from 140 K to 300 K we conclude that the triplet lifetime depends only weakly on sample temperature as long as the temperature stays below the phase transition temperature of 260 K. In ordered films of C_{60} the triplet exciton population decays thus significantly slower than is suggested by ESR measurements on single molecules dissolved in frozen solutions of benzonitrile.[27]

The energy distribution shows a feature between 1.1 eV and 1.3 eV with a lifetime of up to $\tau = 220$ μs, which is interpreted as originating from trapped triplet exciton states of C_{60}. When increasing the sample temperature from 140 K to 295 K a systematic decrease of the lifetime is found. In Fig. 7 the decay rate is plotted as a function of inverse sample temperature. The linear dependence suggests that an interaction between the trapped triplet exciton and phonons leads to a decrease of that lifetime. It may be justified to assume for

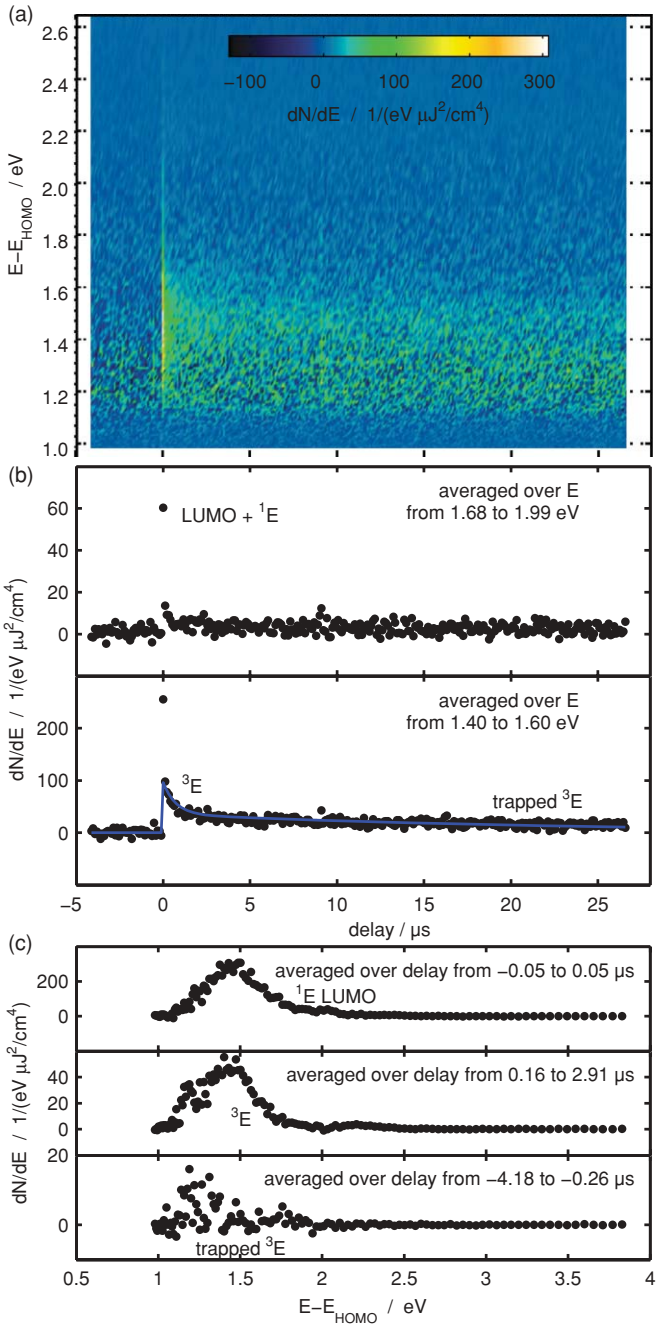

FIG. 6. (a) Energy-time delay plot for two-colour 2PPE at long delay times. Pump photon energy $h\nu = 3.50$ eV ($\lambda = 355$ nm), pump pulse duration 100 ns; probe photon energy $h\nu = 5.88$ eV ($\lambda = 211$ nm), probe photon duration less than 100 ps. (b) The signal averaged over the energy from 1.4 to 1.6 eV is fitted by a superposition of two exponential decays with a lifetime of (720 ± 50) ns and (22.3 ± 0.6) μs. (c) Energy distributions at certain delay times show in the upper trace the excitation of the LUMO and fast population of the ^{1}E, in the middle trace the free ^{3}E, and in the lower trace the trapped ^{3}E. Note that the data shown in the lower trace represent delay times of nearly 1 ms.

the exciton-phonon coupling a similar mechanism as is applied to electron-phonon coupling, and which is described by the Eliashberg formalism.[59] In the high temperature limit this leads to a phonon contribution to the spectral widths of a state according to

$$\Gamma_{\text{ex-ph}} = 2\pi k T \lambda_{\text{ex-ph}}, \quad (6)$$

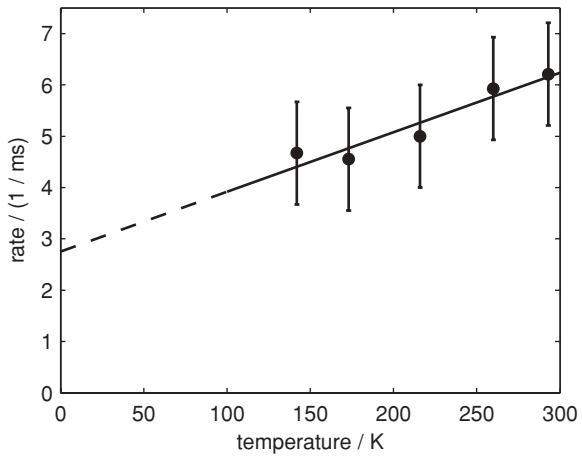

FIG. 7. Decay rate of trapped triplet excitons for various sample temperatures. The slope yields an exciton-phonon coupling of $\lambda_{ex\text{-}ph} = 1.77 \cdot 10^{-10}$. A cautious extrapolation to low temperatures yields a lifetime of about 360 μs.

where $\lambda_{ex\text{-}ph}$ is the exciton-phonon coupling constant. Transposed to the interaction of excitons and phonons the decay rate of trapped triplet exciton states increases linearly with T. From the slope we obtain for the exciton-phonon coupling constant $\lambda_{ex\text{-}ph} = 1.77 \cdot 10^{-10}$. Although this value seems to be very small, however, due to the long lifetime of trapped triplet excitons it has a similar effect on a relative reduction of lifetime as an electron-phonon coupling constant $\lambda_{e\text{-}ph}$ of the order of one commonly observed for electronic metal surface states with lifetimes on the order of 10 fs.

These measurements on the phonon coupling constant were performed on a sample with intentionally higher defect density, as was indicated by a less deep separation between HOMO-1 and HOMO in the 150 nm UPS (see Fig. 2). This was desirable in this case to observe the trapped triplet excitons with sufficient signal-to-noise ratio. Increasing the temperature leads to an increasing decay rate of the excitons. The lifetimes of the free excitons are reduced to around 10 μs at $T = 140$ K and decrease even to a few microseconds around room temperature. These short lifetimes are, however, not representative for free triplet excitons in well-prepared samples, as the other measurements have shown.

IV. CONCLUSION

Long lifetimes in the nanosecond and tens of microsecond range for singlet and triplet excitonic states, respectively, are observed in thin, ordered layers of C_{60} on Cu(111), featuring bulklike properties. This compares well with lifetimes found in isolated C_{60} molecules. Exciton diffusion to the supporting metal surface turns out to be slow at $T_S = 140$ K. Increasing the temperature reveals a phononic coupling of the excitons. The exciton population in the film decays at higher temperatures much slower than suggested by earlier ESR measurements on single molecules dissolved in frozen solutions of host molecules.

ACKNOWLEDGMENTS

This work was partially supported by the Deutsche Forschungsgemeinschaft in project Za 110/21 via the Priority Program SPP 1093. Dynamik von Elektronentransferprozessen an Grenzflächen which is gratefully acknowledged.

[1] N. S. Saricifti, L. Smilowitz, A. J. Heeger, and F. Wudl, Science **258**, 1474 (1992).
[2] H. Imahori, T. Azuma, A. Ajavakom, H. Norieda, H. Yamada, and Y. Sakata, J. Phys. Chem. B **103**, 7233 (1999).
[3] M. S. Dresselhaus, G. Dresselhaus, and P. C. Eklund, *Science of Fullerenes and Carbon Nanotubes* (Academic Press, San Diego, 1996).
[4] G. Gensterblum, J. Elect. Spec. Rel. Ph. **81**, 89 (1995).
[5] P. A. Brühwiler, A. J. Maxwell, P. Rudolf, C. D. Gutleben, B. Wästenberg, and N. Mårtensson, Phys. Rev. Lett. **71**, 3721 (1993).
[6] J. P. Long, S. J. Chase, and M. N. Kabler, Chem. Phys. Lett. **347**, 29 (2001).
[7] R. Jacquemin, S. Kraus, and W. Eberhardt, Sol. State Comm. **105**, 449 (1998).
[8] S. Link, A. Scholl, R. Jacquemin, and W. Eberhardt, Sol. State Comm. **113**, 689 (2000).
[9] J. P. Long, S. J. Chase, and M. N. Kabler, Phys. Rev. B **64**, 205415 (2001).
[10] A. G. Stepanov, M. T. Portella-Oberli, A. Sassara, and M. Chergui, Chem. Phys. Lett. **358**, 516 (2002).
[11] G. Dutton and X.-Y. Zhu, J. Phys. Chem. B **108**, 7788 (2004).
[12] O. Echt, S. Yao, and R. Deng, J. Phys. Chem. A **108**, 6944 (2004).
[13] E. E. B. Campbell, G. Ulmer, and I. V. Hertel, Phys. Rev. Lett. **67**, 1986 (1991).
[14] Y. Wang, J. M. Holden, A. M. Rao, P. C. Eklund, U. D. Venkateswaran, D. Eastwood, R. L. Lidberg, G. Dresselhaus, and M. S. Dresselhaus, Phys. Rev. B **51**, 4547 (1995).
[15] T. Ohno, Y. Chen, S. Harvey, G. H. Kroll, J. H. Weaver, R. E. Haufler, and R. E. Smalley, Phys. Rev. B **44**, 13747 (1991).
[16] J.-M. Themlin, S. Bouzidi, F. Coletti, J.-M. Debever, G. Gensterblum, Li-Ming Yu, J.-J. Pireaux, and P. A. Thiry, Phys. Rev. B **46**, 15602 (1992).
[17] G. Gensterblum, J.-J. Pireaux, P. Thiry, R. Caudano, T. Buslaps, R. L. Johnson, G. Lee Lay, V. Aristov, R. Günther, A. Taleb-Ibrahimi, G. Indlekofer, and Y. Petrov, Phys. Rev. B **48**, 14756 (1993).
[18] A.-M. Janner, H. T. Jonkman, and G. A. Sawatzky, Phys. Rev. B **63**, 085111 (2001).
[19] R. Könenkamp, R. Engelhardt, and R. Henninger, Sol. State Comm. **97**, 285 (1996).
[20] G. Gensterblum, J.-J. Pireaux, P. A. Thiry, R. Caudano, J. P. Vigneron, Ph. Lambin, A. A. Lucas, and W. Krätschmer, Phys. Rev. Lett. **67**, 2171 (1991).
[21] K. Kuhnke, R. Becker, M. Epple, and K. Kern, Phys. Rev. Lett. **79**, 3246 (1997).
[22] A. Watanabe, O. Ito, M. Watanabe, H. Saito, and M. Koishi, Chem. Commun. **173**, 117 (1996).
[23] M. R. Wasielewski, M. P. O'Neil, K. R. Lykke, M. J. Pellin, and D. M. Gruen, J. Am. Chem. Soc. **113**, 2774 (1991).
[24] J. W. Arbogast, C. S. Foote, and M. Kao, J. Am. Chem. Soc. **114**, 2277 (1992).
[25] A. Sassara, G. Zerza, and M. Chergui, Chem. Phys. Lett. **261**, 213 (1996).
[26] W.-C. Hung, C.-D. Ho, C.-P. Liu, and Y.-P. Lee, J. Phys. Chem. **100**, 3927 (1996).
[27] M. Bennati, A. Grupp, M. Mehring, K. P. Dinse, and J. Fink, Chem. Phys. Lett. **200**, 440 (1992).
[28] M. Hedén, A. V. Bulgakov, K. Mehlig, and E. E. B. Campbell. J. Chem. Phys. **118**, 16 (2003).
[29] A. Tamai, A. P. Seitsonen, F. Baumberger, M. Hengsberger, Z.-X. Shen, T. Greber, and J. Osterwalder, Phys. Rev. B **77**, 075134 (2008).
[30] K.-D. Tsuei and P. D. Johnson, Sol. State Comm. **101**, 337 (1996).
[31] K.-D. Tsuei, J.-Y. Yuh, C.-T. Tzeng, R.-Y. Chu, S.-C. Chung, and K.-L. Tsang, Phys. Rev. B **56**, 15412 (1997).
[32] L.-L. Wang and H.-P. Cheng, Phys. Rev. B **69**, 045404 (2004).
[33] X. Lu, M. Grobis, K. H. Khoo, S. G. Louie, and M. F. Crommie, Phys. Rev. B **70**, 115418 (2004).
[34] A. Popović, G. Dražič, and J. Marsel, Rapid Commun. Mass Spectrometry **8**, 985 (1994).

[35]D. M. Poirier, D. W. Owens, and J. H. Weaver, Phys. Rev. B **51**, 1830 (1995).
[36]K. Finsterbusch, R. Urschel, and H. Zacharias, Appl. Phys. B **70**, 741 (2000).
[37]K. Finsterbusch, R. Urschel, and H. Zacharias, Appl. Phys. B **74**, 319 (2002).
[38]K. Finsterbusch, A. Bayer, and H. Zacharias, Appl. Phys. B **79**, 457 (2004).
[39]R. Hilbig and R. Wallenstein, IEEE J. Quantum Electron. **QE-17**, 1566 (1981).
[40]J. Kutzner and H. Zacharias, Appl. Phys. B **66**, 571 (1998).
[41]R. W. Lof, M. A. van Veenendaal, B. Koopmans, H. T. Jonkman, and G. A. Sawatzky, Phys. Rev. Lett. **68**, 3924 (1992).
[42]M. R. C. Hunt, P. Rudolf, and S. Modesti, Phys. Rev. B **55**, 7889 (1997).
[43]P. O. Gartland, S. Berge, and B. J. Slagsvold, Phys. Rev. Lett. **28**, 738 (1972).
[44]G. Dutton and X.-Y. Zhu, J. Phys. Chem. B **106**, 5975 (2002).
[45]P. Rudolf, M. S. Golden, and P. A. Brühwiler, J. Elect. Spec. Rel. Ph. **100**, 409 (1999).
[46]A. Goldoni, C. Cepek, and S. Modesti, Phys. Rev. B **54**, 2890 (1996).
[47]S. L. Ren, Y. Wang, A. M. Rao, E. McRae, J. M. Holden, T. Hager, K. Wang, W.-T. Lee, H. F. Ni, J. Selegue, and P. C. Eklund, Appl. Phys. Lett. **59**, 2678 (1991).
[48]A.-M. Janner, R. Eder, B. Koopmans, H. T. Jonkman, and G. A. Sawatzky, Phys. Rev. B **52**, 17158 (1995).
[49]R. Könenkamp, G. Priebe, and B. Pietzak, Phys. Rev. B **60**, 11804 (1999).
[50]B. Mishori, Y. Shapira, A. Belu-Marian, M. Manciu, and A. Devenyi, Chem. Phys. Lett. **264**, 163 (1997).
[51]S. Kazaoui, N. Minami, Y. Tanabe, H. J. Byrne, A. Eilmes, and P. Petelenz, Phys. Rev. B **58**, 7689 (1998).
[52]W. Guss, J. Feldmann, E. O. Göbel, C. Taliani, H. Mohn, W. Müller, P. Häussler, and H.-U. ter Meer, Phys. Rev. Lett. **72**, 2644 (1994).
[53]D. J. Van Den Heuvel, I. Y. Chan, E. J. J. Groenen, J. Schmidt, and G. Meijer, Chem. Phys. Lett. **231**, 111 (1994).
[54]H. J. Byrne, W. Maser, W. W. Rühle, A. Mittelbach, W. Hönle, H. G. von Schnering, B. Movaghar, and S. Roth, Chem. Phys. Lett. **204**, 461 (1993).
[55]E. L. Shirley, L. X. Benedict, and S. G. Louie, Phys. Rev. B **54**, 10970 (1996).
[56]E. L. Shirley and S. G. Louie, Phys. Rev. Lett. **71**, 133 (1993).
[57]K. Kuhnke, R. Becker, and K. Kern, Chem. Phys. Lett. **257**, 569 (1996).
[58]K. Thonke, R. Schliesing, N. Teofilov, H. Zacharias, R. Sauer, A. M. Zaitsev, H. Kanda, and T. R. Anthony, Diamond Rel. Mater. **9**, 428 (2000).
[59]A. Eiguren, B. Hellsing, E. V. Chulkov, and P. M. Echenique, Phys. Rev. B **67**, 235432 (2003).